

# Accelerating Inference of Masked Image Generators via Reinforcement Learning

Pranav Subbaraman\*, Shufan Li\*, Siyan Zhao, Aditya Grover

UCLA

pranavs108@ucla.edu, jacklishufan@cs.ucla.edu

siyanz@ucla.edu, adityag@cs.ucla.edu

\*Equal Contribution



Figure 1. Speed-RL is a framework for masked generative models to generate high quality images while using significantly fewer steps. Specifically, Speed-RL uses reinforcement learning to optimize a speed and quality reward.

## Abstract

*Masked Generative Models (MGM)s demonstrate strong capabilities in generating high-fidelity images. However, they need many sampling steps to create high-quality generations, resulting in slow inference speed. In this work, we propose Speed-RL, a novel paradigm for accelerating a pretrained MGMs to generate high-quality images in fewer steps. Unlike conventional distillation methods which formulate the acceleration problem as a distribution matching problem, where a few-step student model is trained to*

*match the distribution generated by a many-step teacher model, we consider this problem as a reinforcement learning problem. Since the goal of acceleration is to generate high quality images in fewer steps, we can combine a quality reward with a speed reward and finetune the base model using reinforcement learning with the combined reward as the optimization target. Through extensive experiments, we show that the proposed method was able to accelerate the base model by a factor of 3x while maintaining comparable image quality.*

## 1. Introduction

Diffusion models have been shown to generate high-quality images from text prompts [23, 25, 26, 36]. A new framework, Masked generative models (MGMs), has recently emerged as a powerful class of models for a wide range of generative tasks [1, 4, 12, 31]. MGMs have been widely applied in producing high-quality image generation [2, 4, 5, 12, 22]. They have also been successfully applied to video generation [10, 34] and text generation [8, 11, 19, 21]. Despite these strengths, MGMs typically require many sampling steps to produce high quality images, which makes real-time or low-latency applications impractical. Therefore, reducing the number of sampling steps presents an impactful opportunity. If we can preserve generation quality while cutting inference cost, MGMs become far more useful in production settings ranging from interactive content creation to on-device synthesis.

Most prior work on accelerating generative diffusion models frames the problem as a distillation or distribution-matching problem. These methods train a compact, few-step student to emulate a many-step teacher. While effective in some settings, these approaches are limited by the need to explicitly model the teacher’s distribution and by instability when the student’s sampling trajectories diverge from those seen during teacher training. For discrete, high entropy token distributions typical of masked image generators, sample-based estimators for divergence (e.g. naive KL estimators) suffer from high variance, which can destabilize training and limit the potential benefits of direct distillation.

In parallel, reinforcement learning (RL) has recently been used to fine-tune generative models by directly optimizing human preference or quality-based rewards [15, 38]. These works suggest that the direct optimization quality and inference cost via RL is a promising direction for high performance generation.

In this work, we take a different view. That is, accelerating a pretrained MGM by directly optimizing for the downstream objective of high image quality and low sampling cost using reinforcement learning. We introduce Speed-RL, a framework that combines a task-level quality reward (e.g. ImageReward [37], HPSv2 [35], CLIP [24]) with an explicit speed reward that favors shorter sampling trajectories. To make policy optimization stable in the discrete, high entropy setting of MGMs, we adapt group-ratio policy optimization (GRPO) [30] with a low-variance KL regularizer and a cross-entropy based estimator that more faithfully captures the full token distribution rather than relying only on sampled tokens. This combination produces stable, directed fine-tuning of the base model toward concise, high quality generation trajectories.

We conduct extensive experiments to test the effectiveness of Speed-RL. We show that Speed-RL can accelerate the base model by a factor of 3x while maintaining percep-

tual and reward-driven quality metrics.

Our main contributions include:

- We cast the problem of accelerating discrete masked diffusion models as a reinforcement learning problem and propose a combined quality + speed reward that directly optimizes the practical objective of interest.
- We adapt GRPO for high entropy discrete generators by introducing a low-variance KL estimator based on cross-entropy terms, improving training stability for MGMs.
- We empirically validate Speed-RL on a 1B-parameter Meissson base model [2] and show that it achieves up to 3x inference speedups with comparable ImageReward, HPSv2.1, and CLIP scores. We include extensive ablation studies that isolate the effects of different hyperparameters.

## 2. Related Works

### 2.1. Diffusion Model Acceleration

Diffusion models have demonstrated remarkable generative performance across modalities, but their iterative sampling process leads to slow inference. Prior works have sought to accelerate diffusion-based generation through distillation and model compression [27, 32]. Other works reformulate diffusion as flow matching to reduce the number of integration steps [7, 18]. However, these approaches depend on accurate distribution matching between teacher and student models, which can be unstable. This is particularly true for discrete masked diffusion models where high entropy token distributions make divergence estimation noisy.

### 2.2. Masked Generative Models

MGMs such as MaskGIT [4] and MUSE [5] replace the continuous denoising process of diffusion with discrete token prediction. This leads to parallel decoding and improved sample quality. Subsequent works like Meissson [2] and MaskDiT [40] extended these models with diffusion-style iterative unmasking, achieving strong text-to-image fidelity. Despite their efficiency relative to standard diffusion, MGMs still require many sampling steps to reach optimal quality. This motivates our work on direct optimization of speed-quality tradeoffs.

### 2.3. Reinforcement Learning for Generative Models

Recent advances in RL fine-tuning of generative models have shown that non-differentiable quality metrics, such as human preference, can guide large model behavior beyond likelihood training. In text generation, PPO [29] and GRPO [30] have been used to align model outputs with human evaluations. In image generation, ImageReward [37] and HPSv2.1 [35] introduced learned aesthetic and preference rewards for text-to-image models. These methods suggest that RL can be used not only for preference alignment but

also for task-specific objectives (e.g. inference efficiency).

## 2.4. Reinforcement Learning for Diffusion Model Optimization

Recent works on using RL to fine-tune diffusion models can be grouped into three broad themes: alignment and preference optimization [3, 13, 16], efficiency and inference-speed optimization [20, 39], and structural/control applications where diffusion models serve in RL or planning roles [9, 41]. Unlike prior RL works that focus on alignment or adapting the generative process for control, we make inference cost (step count and latency) an explicit optimization objective and directly reward shorter, high quality generation trajectories. Furthermore, we jointly optimize architecture-level decisions (step schedules, masking policy) together with reward design and introduce stable RL adaptations for high entropy, discrete token generators. This allows for significant reduction in sampling steps that prior methods do not target.

## 3. Method

We formulate the acceleration problem of discrete diffusion model as a reinforcement learning problem. Given a prompt  $c$ , a sampled diffusion trajectories  $\{x_t\} = \{x_T, x_{T-1}..x_0\}$  from a masked diffusion model(MDM)  $p_\theta$ , with  $x_t$  being a fully masked image and  $x_0$  a clean image, our goal is to solve the following optimization objective

$$\max \mathbb{E}_{x_0 \sim p_\theta(x_0|c), c \sim \mathcal{D}} [R(x_0, c) + \frac{\tau}{|\{x_t\}|}] \quad (1)$$

where  $R(x_0, c)$  is a real-valued reward function computed over pairs of prompts and generative images,  $\{x_t\}$  is the number of sampling steps, and  $\tau$  is a scaling factor. The term  $\frac{\tau}{|\{x_t\}|}$  serves as a ‘‘speed reward’’ that increases as the number of sampling steps  $\{x_t\}$  decreases. The hyperparameter  $\tau$  controls the relative contribution of the speed reward to the whole learning process.

### 3.1. Improving GRPO’s Stability

We employ GRPO as our reinforcement learning framework. However, there are some unique challenges in applying it to masked image generators. Recall that the standard GRPO contains a KL penalty term computed using the following estimator:

$$\mathbb{D}_{\text{KL}}[p_\theta \| p_{\text{ref}}] = \frac{p_{\text{ref}}(x_i | c)}{p_\theta(x_i | c)} - \log \frac{p_{\text{ref}}(x_i | c)}{p_\theta(x_i | c)} - 1, \quad (2)$$

over a group of generated samples  $x_1, \dots, x_G$ . However, this estimator only uses actual sampled tokens instead of the whole token distribution produced by  $p_{\text{ref}}$ . In discrete image generators,  $p_{\text{ref}}$  typically has higher entropy than language tasks, with more high likelihood candidates. Using

only sampled token in this case leads to high variance and potentially instability in the tail region of the distribution. To address this, we can replace the estimator based on the relation

$$\mathbb{D}_{\text{KL}}[p_\theta \| p_{\text{ref}}] = H(p_{\text{ref}}|p_\theta) - H(p_{\text{ref}}) \quad (3)$$

where  $H(p_\theta|p_{\text{ref}})$  is the cross entropy and  $H(p_{\text{ref}})$  is the entropy.

With this adaptation, we can use the following final learning objective in place of GRPO loss

$$\begin{aligned} \mathcal{L}_{\text{Speed-RL}} = & A_i L_{\text{ce}}(\mathbf{x}_i, p_\theta(X_i | c_i)) \\ & + \beta L_{\text{ce}}(p_{\text{ref}}(X_i | c_i), p_\theta(X_i | c_i)) \end{aligned} \quad (4)$$

where  $A_i$  is the group advantage term in GRPO,  $L_{\text{ce}}$  is the cross entropy loss,  $p(X_i | c_i)$  are per-token probability vector and  $\mathbf{x}_i$  is a one-hot vector. We will show that this approach result in the same gradient as the vanilla GRPO loss with our proposed KL divergence estimator. We will provide a full proof in the appendix.

### 3.2. Low Quality Sample Filtering

We employ a technique to filter out prompts where the reward model shows high variance and uncertainty in its scoring. The overall method is as follows. First, we generate multiple samples for each prompt. Then, we score each sample with a reward model. Next, we calculate the standard deviation of the reward scores for that prompt, and then filter out prompts where the standard deviation is greater than a threshold.

More formally, The filtering mechanism detects and rejects ‘‘low-diversity’’ batches where generated samples have similar quality (low variance in rewards). Such batches provide weak learning signals because:

- Weak advantage signals: GRPO relies on reward differences to compute advantages. If all samples have similar rewards, advantages become noisy.
- Poor exploration: Low variance indicates the model is producing repetitive outputs, limiting exploration of the reward landscape.
- Inefficient learning: Training on uniform-quality batches wastes compute without teaching the model meaningful distinctions.

#### Step 1: Batch Generation and Reward Computation

For a given prompt, the system generates a batch of images with varying inference steps:

- Images:  $\{x_1, x_2, \dots, x_n\}$  where  $n = \text{batch\_size}$
- Rewards:  $R = \{r_1, r_2, \dots, r_n\}$  where  $r_i = f_{\text{reward}}(x_i, \text{prompt})$

The final score includes speed rewards:

$$r_i = r_{\text{base}}(x_i) + \alpha \cdot \left( \frac{8}{\text{nfe}_i} \right)$$

where  $\alpha$  is speed\_reward\_factor and  $\text{nfe}_i$  is the number of function evaluations for sample  $i$ .

### Step 2: Standard Deviation Calculation

For multi-GPU training, rewards are gathered across all GPUs:

$$R_{\text{all}} = [R^{(0)}, R^{(1)}, \dots, R^{(k-1)}] \quad \%k \text{ GPUs}$$

The reward standard deviation is computed:

$$\sigma_{\text{batch}} = \text{mean}(\{\text{std}(R^{(0)}), \text{std}(R^{(1)}), \dots, \text{std}(R^{(k-1)})\})$$

### Step 3: Historical Tracking and Percentile Threshold

The system maintains a sliding window of historical standard deviations:

$$H = \{\sigma_1, \sigma_2, \dots, \sigma_m\} \text{ where } m \leq \text{history\_size}$$

Default: history\_size = 100

The acceptance threshold is the  $p$ -th percentile of historical values:

$$\tau = \text{percentile}(H, p)$$

Default:  $p = 10$  (10th percentile - only batches with std dev in the bottom 10% are rejected)

### Step 4: Accept/Reject Decision

The batch is accepted if:

$$\sigma_{\text{batch}} \geq \tau \quad \text{OR} \quad \text{resample\_attempts} > \text{max\_attempts}$$

Otherwise, regenerate the entire batch and recompute.

### Step 5: History Update

After acceptance, update the sliding window:

$$H \leftarrow H \cup \{\sigma_{\text{batch}}\}$$

if  $|H| > \text{history\_size}$ :

$$H \leftarrow H[1:] \quad \% \text{ Remove oldest}$$

In this way, we keep only low variance prompts for training. Overall, this can help identify problematic prompts since high standard deviation indicates the reward model is uncertain about how to score that prompt. We can improve the training data quality by removing these prompts. We see more consistent and reliable reward signals when evaluating models after using this technique. This design is inspired by VCRL which uses this for language [14].

## 4. Experiment Results

### 4.1. Setup

#### 4.1.1. Dataset

We sample 100k prompts from LAION-Aesthetics [28], BLIP3O-60k [6]

#### 4.1.2. Reward Models

We set up a pipeline to use Meissonic [2], a foundational text-to-image MGM with 1B parameters, to generate images for evaluating different reward model options. We sample 20 prompts from BLIP3o-60k and generate 100 images each using 16, 32, and 48 sampling steps. We then run the ImageReward, PickScore, HPSv2.1, and CLIP on each of these generated images. We visually inspect the top-k scored images for different prompts for each reward model and calculate average scores and standard deviations for each reward model across steps. Based on this analysis, we decide that for a given reward model, an image generated by our framework is high quality if it gets a score greater than or equal to one standard deviation above the average score for the baseline model’s generations. We establish that an image generated by our framework is low quality if it gets a score below the average score for the baseline model’s generations. Overall, this helps us evaluate the quality of different reward models and determine thresholds for high quality and low quality images generated by our framework.

#### 4.1.3. Training

We train the base model using our modified GRPO objective. We use a global batch size of 96 and across 8 GPUs and a learning rate of  $5 \times 10^{-7}$  for 1500 steps.

### 4.2. Qualitative Results

We report qualitative comparisons in Fig. 2. We compare text-to-image generations of Speed-RL with 16 sampling steps and compare it with generations from baseline model Meissonic at 16, 32, and 48 steps on HPSv2.1 dataset. These visual results demonstrate that Speed-RL was able to achieve comparable generation quality with a  $4\times$  speedup.

### 4.3. Main Results

We report results on the HPSv2.1 benchmark and the PartiPrompts benchmark in Table 1. We employ ImageReward, HPSv2.1, and CLIP PickScore score as our quality reward models. We compare these metrics of the base model and finetuned model under different sampling steps. Speed-RL delivers quality on par with the baseline across both benchmarks and all three reward models, while achieving a  $3\times$  speedup, requiring only one-third of the sampling steps used by the baseline.

These results show that with RL finetuning, we can obtain higher image quality than the base model while also



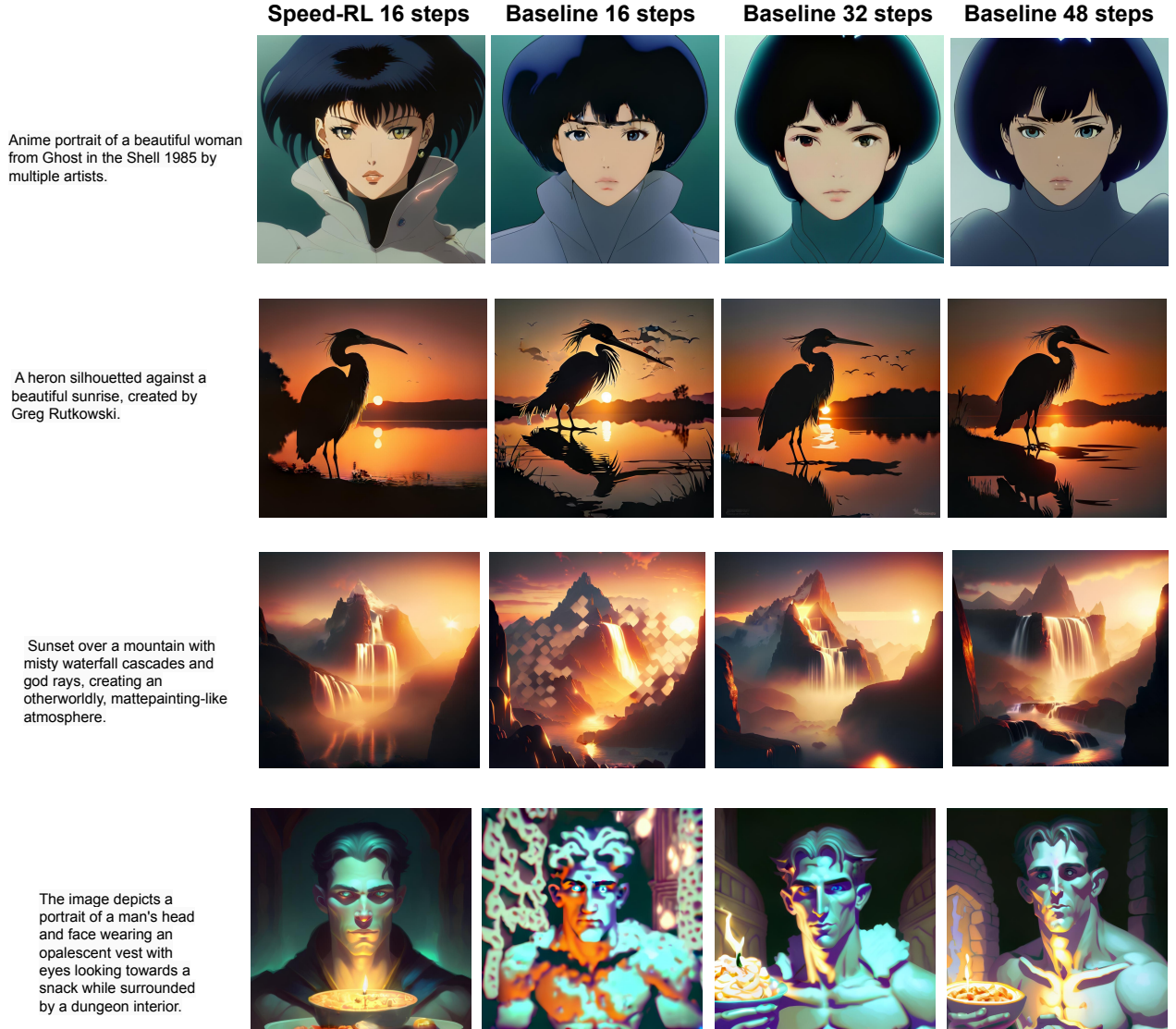


Figure 2. **Side-by-side qualitative comparison of Speed-RL and Meisssonic (baseline).** Speed-RL produces higher quality images while using significantly fewer steps.

achieving a speedup of 3x. We observe that the improvements in low-sampling steps is more significant, which may be an effect of our speed reward that focus the positive learning signal on generations with fewer steps.

#### 4.4. Ablation Studies

We measure the effect of various design choices by conducting thorough ablation studies on Speed-RL.

##### 4.4.1. Speed Reward and KL Regularizer

In Figure 3, we visualize the average reward of generated samples throughout the training process on 16-step generations. We find that without speed reward, the training converges slower as less positive advantages are assigned to samples with fewer steps. Without our proposed change to the KL regularizer, the training diverges, highlighting the instability problems with vanilla sample-based KL estimator.

HPS Benchmark				PartiPrompts Benchmark			
Model	Steps	ImageReward	PickScore	Model	Steps	ImageReward	PickScore
Meissonic	48	41.901	21.416	Meissonic	48	28.903	21.498
Speed-RL	<b>16</b>	<b>63.346</b>	<b>21.607</b>	Speed-RL	<b>16</b>	<b>45.947</b>	<b>21.394</b>
Speed-RL	32	69.019	21.682	Speed-RL	32	43.349	21.414
Speed-RL	48	64.485	21.611	Speed-RL	48	34.522	21.335

Table 1. Comparison of Meissonic and Speed-RL across HPSv2.1 and PartiPrompts benchmarks. Across both benchmarks and all reward models, Speed-RL matches baseline quality and achieves a 3 $\times$  speedup using only one-third of the sampling steps.

Model	Step	Anime	Concept Art	Paintings	Photo	Overall
Baseline	48	27.469	25.357	25.248	22.835	25.227
Speed-RL	<b>16</b>	<b>28.457</b>	<b>27.849</b>	<b>26.581</b>	<b>24.491</b>	<b>26.845</b>
Speed-RL	32	29.169	27.411	26.926	24.701	27.052
Speed-RL	48	28.821	27.139	26.741	24.551	26.813

Table 2. HPSv2.1 Scores Comparison (Speed-RL vs. Baseline) by Category. Speed-RL’s overall HPSv2.1 score is +1.618 than the baseline model’s score while using only 16 steps compared to 48. The ConceptArt and Photo categories show the greatest improvement.

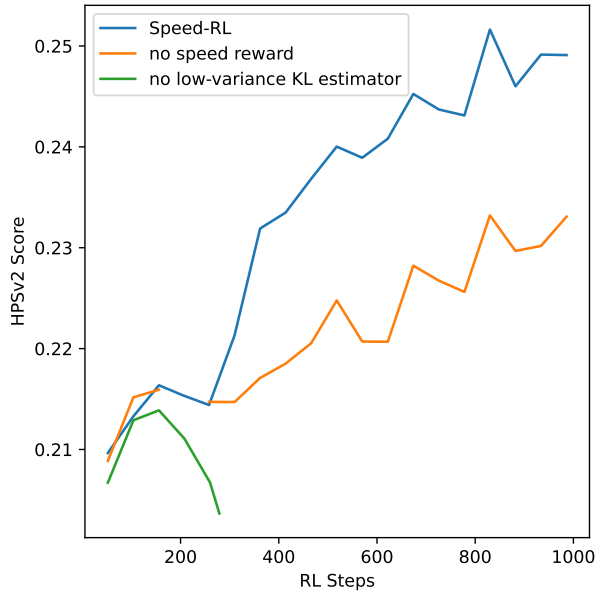


Figure 3. Ablation study on our speed reward and KL regularizer. We see a divergence in HPSv2.1 scores after 300 RL steps, where Speed-RL increases faster compared to having no speed reward and no low-variance KL estimator.

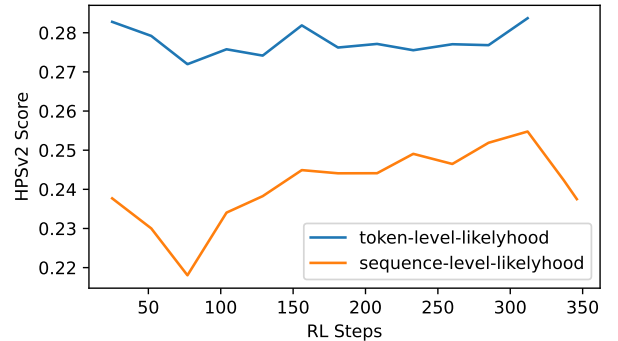


Figure 4. Ablation study on the effect of enabling per-token-likelihood. There is a gap between using token-level-likelihood and sequence-level-likelihood where using token-level-likelihood consistently has a HPSv2.1 score higher than using sequence-level-likelihood.

#### 4.4.2. Enabling Per Token Likelihood

We experiment with both including and not including per-token-likelihood where all other hyperparameters are held constant. We observe that not including per-token-likelihood results in a higher average HPSv2.1 reward score across over 300 steps and thus we do not include per-token-likelihood in our optimal selection of hyperparameter values (Figure 4).

Model	Step	Abstract	Animals	Artifacts	Arts	Food & Bev.	Illustrations	Indoor	Outdoor	Overall
Baseline	48	18.210	28.239	24.528	25.922	22.165	24.703	23.410	23.137	23.763
Speed-RL	<b>16</b>	<b>22.329</b>	<b>28.895</b>	<b>24.459</b>	<b>27.887</b>	<b>21.987</b>	<b>24.756</b>	<b>25.294</b>	<b>24.669</b>	<b>22.252</b>
Speed-RL	32	21.551	29.448	24.349	27.901	20.977	24.548	25.793	24.937	24.888
Speed-RL	48	21.017	29.083	23.949	28.013	20.389	24.224	25.322	24.258	24.488

Table 3. PartiPrompts Benchmark HPSv2.1 Scores (Speed-RL vs. Baseline) by Category. Speed-RL achieves a very comparable HPSv2.1 reward score with **3x** fewer steps than the baseline.

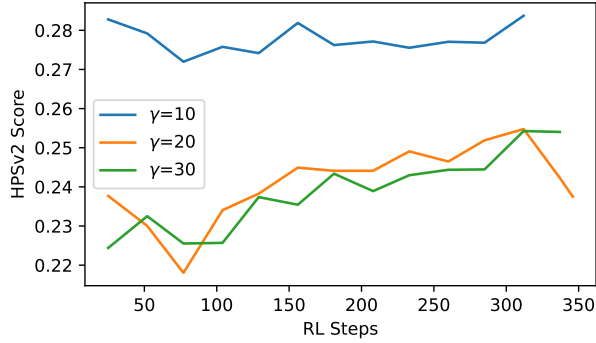


Figure 5. Ablation study on varying the reward standard deviation percentile threshold.

#### 4.4.3. Low Quality Sample Filtering

We try a low-quality sample filtering method. This tracks the historical standard deviation of rewards within each group of generations, and if a newly generated group has a reward standard deviation below a certain percentile threshold, it discards and resamples that entire group. We measure the effect of different percentile threshold values for this method, and observe that as the threshold increases, the average HPSv2.1 reward becomes increasingly noisy. We choose 10.0 percent for our threshold value to strike a balance between very high noise and filtering too few groups.

#### 4.4.4. Number Of Gradient Update Steps Per Batch

We vary the number of gradient update steps per batch of generated images. A higher value results in better sample efficiency and fewer image generation calls (faster training, less compute). However, this means optimizing on "stale" samples, i.e. the policy updates but keep training on old generations. This also has a risk of overfitting. On the other hand, lower values result in more frequent image generation with updated policy (fresher samples). This means better alignment between current policy and training data at the cost of slower training overall (more compute for generation). We find that setting this value to 1 at the cost of slower training time gets the best performance.

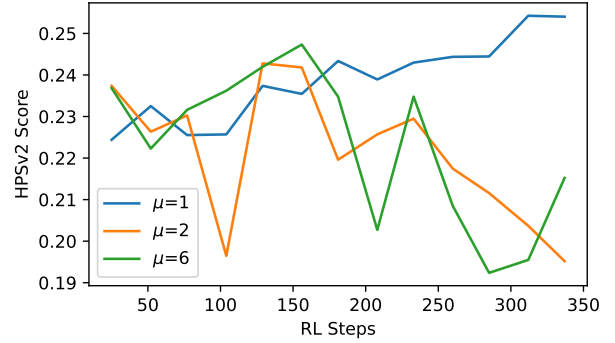


Figure 6. Ablation study on varying the number of gradient update steps per batch.

#### 4.4.5. CFG Value

We try different Classifier-Free Guidance (CFG) values and analyze the overall variance and average reward. We prefer relatively higher CFG values to get more diversity in generation.

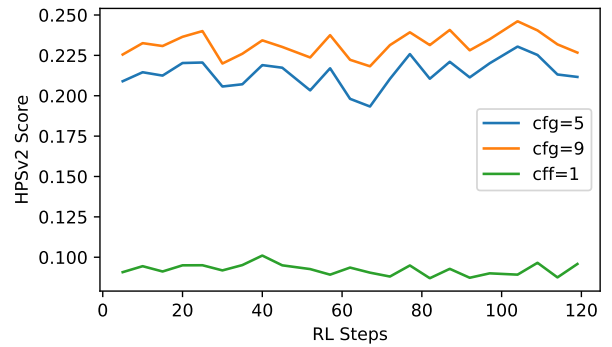


Figure 7. Ablation study on varying the Classifier-Free Guidance (CFG) value.

## 5. Conclusion

In this work, we introduced Speed-RL, a new framework to accelerate masked image generators that moves beyond

distillation and directly optimizes for high quality images produces in minimal sampling steps. By pairing a speed reward with a quality reward and introducing a low variance KL regularizer tailored to MGMs, Speed-RL delivers 3x inference acceleration with no degradation in ImageReward, HPSv2.1, or CLIP metrics across two benchmarks. Our work shows that RL is not only feasible but advantageous for controlling the sampling behavior of discrete diffusion-style models. We believe this represents a promising direction for scalable generative modeling with efficient inference.



## References

- [1] Jacob Austin, Daniel D Johnson, Jonathan Ho, Daniel Tarlow, and Rianne Van Den Berg. Structured denoising diffusion models in discrete state-spaces. *Advances in neural information processing systems*, 34:17981–17993, 2021. 2
- [2] Jinbin Bai, Tian Ye, Wei Chow, Enxin Song, Qing-Guo Chen, Xiangtai Li, Zhen Dong, Lei Zhu, and Shuicheng Yan. Meissonic: Revitalizing masked generative transformers for efficient high-resolution text-to-image synthesis. In *The Thirteenth International Conference on Learning Representations*, 2024. 2, 4
- [3] Kevin Black, Michael Janner, Yilun Du, Ilya Kostrikov, and Sergey Levine. Training diffusion models with reinforcement learning, 2024. 3
- [4] Huiwen Chang, Han Zhang, Lu Jiang, Ce Liu, and William T Freeman. Maskgit: Masked generative image transformer. In *Proceedings of the IEEE/CVF conference on computer vision and pattern recognition*, pages 11315–11325, 2022. 2
- [5] Huiwen Chang, Han Zhang, Jarred Barber, AJ Maschinot, Jose Lezama, Lu Jiang, Ming-Hsuan Yang, Kevin Murphy, William T Freeman, Michael Rubinstein, et al. Muse: Text-to-image generation via masked generative transformers. *arXiv preprint arXiv:2301.00704*, 2023. 2
- [6] Jiahai Chen, Zhiyang Xu, Xichen Pan, Yushi Hu, Can Qin, Tom Goldstein, Lifu Huang, Tianyi Zhou, Saining Xie, Silvio Savarese, et al. Blip3-o: A family of fully open unified multimodal models-architecture, training and dataset. *arXiv preprint arXiv:2505.09568*, 2025. 4, S2
- [7] Quan Dao, Hao Phung, Trung Tuan Dao, Dimitris N Metaxas, and Anh Tran. Self-corrected flow distillation for consistent one-step and few-step image generation. In *Proceedings of the AAAI Conference on Artificial Intelligence*, pages 2654–2662, 2025. 2
- [8] Justin Deschenaux and Caglar Gulcehre. Beyond autoregression: Fast llms via self-distillation through time. *arXiv preprint arXiv:2410.21035*, 2024. 2
- [9] Xiaoyi Dong, Jian Cheng, and Xi Sheryl Zhang. Maximum entropy reinforcement learning with diffusion policy, 2025. 3
- [10] Michael Fuest, Vincent Tao Hu, and Björn Ommer. Mask-flow: Discrete flows for flexible and efficient long video generation. *arXiv preprint arXiv:2502.11234*, 2025. 2
- [11] Shansan Gong, Shivam Agarwal, Yizhe Zhang, Jiacheng Ye, Lin Zheng, Mukai Li, Chenxin An, Peilin Zhao, Wei Bi, Jiawei Han, et al. Scaling diffusion language models via adaptation from autoregressive models. *arXiv preprint arXiv:2410.17891*, 2024. 2
- [12] Vincent Tao Hu and Björn Ommer. [mask] is all you need. *arXiv preprint arXiv:2412.06787*, 2024. 2
- [13] Zijiang Hu, Fengda Zhang, and Kun Kuang. D-fusion: Direct preference optimization for aligning diffusion models with visually consistent samples, 2025. 3
- [14] Guochao Jiang, Wenfeng Feng, Guofeng Quan, Chuzhan Hao, Yuewei Zhang, Guohua Liu, and Hao Wang. Vcrl: Variance-based curriculum reinforcement learning for large language models. *arXiv preprint arXiv:2509.19803*, 2025. 4
- [15] Mo Kordzanganeh, Danial Keshvary, and Nariman Arian. Pixel-wise rl on diffusion models: Reinforcement learning from rich feedback. *arXiv preprint arXiv:2404.04356*, 2024. 2
- [16] Preeti Lamba, Kiran Ravish, Ankita Kushwaha, and Pawan Kumar. Alignment and safety of diffusion models via reinforcement learning and reward modeling: A survey, 2025. 3
- [17] Tsung-Yi Lin, Michael Maire, Serge Belongie, Lubomir Bourdev, Ross Girshick, James Hays, Pietro Perona, Deva Ramanan, C. Lawrence Zitnick, and Piotr Dollár. Microsoft coco: Common objects in context, 2015. S2
- [18] Xingchao Liu, Chengyue Gong, and Qiang Liu. Flow straight and fast: Learning to generate and transfer data with rectified flow. *arXiv preprint arXiv:2209.03003*, 2022. 2
- [19] Aaron Lou, Chenlin Meng, and Stefano Ermon. Discrete diffusion modeling by estimating the ratios of the data distribution. *arXiv preprint arXiv:2310.16834*, 2023. 2
- [20] Haitong Ma, Tianyi Chen, Kai Wang, Na Li, and Bo Dai. Efficient online reinforcement learning for diffusion policy, 2025. 3
- [21] Shen Nie, Fengqi Zhu, Zebin You, Xiaolu Zhang, Jingyang Ou, Jun Hu, Jun Zhou, Yankai Lin, Ji-Rong Wen, and Chongxuan Li. Large language diffusion models. *arXiv preprint arXiv:2502.09992*, 2025. 2
- [22] Suraj Patil, William Berman, Robin Rombach, and Patrick von Platen. amused: An open muse reproduction. *arXiv preprint arXiv:2401.01808*, 2024. 2
- [23] Dustin Podell, Zion English, Kyle Lacey, Andreas Blattmann, Tim Dockhorn, Jonas Müller, Joe Penna, and Robin Rombach. Sdxl: Improving latent diffusion models for high-resolution image synthesis. *arXiv preprint arXiv:2307.01952*, 2023. 2
- [24] Alec Radford, Jong Wook Kim, Chris Hallacy, Aditya Ramesh, Gabriel Goh, Sandhini Agarwal, Girish Sastry, Amanda Askell, Pamela Mishkin, Jack Clark, et al. Learning transferable visual models from natural language supervision. In *International conference on machine learning*, pages 8748–8763. PmLR, 2021. 2
- [25] Aditya Ramesh, Mikhail Pavlov, Gabriel Goh, Scott Gray, Chelsea Voss, Alec Radford, Mark Chen, and Ilya Sutskever. Zero-shot text-to-image generation. In *Proceedings of the 38th International Conference on Machine Learning*, pages 8821–8831. PMLR, 2021. 2
- [26] Robin Rombach, Andreas Blattmann, Dominik Lorenz, Patrick Esser, and Björn Ommer. High-resolution image synthesis with latent diffusion models. In *Proceedings of the IEEE/CVF conference on computer vision and pattern recognition*, pages 10684–10695, 2022. 2
- [27] Tim Salimans and Jonathan Ho. Progressive distillation for fast sampling of diffusion models. *arXiv preprint arXiv:2202.00512*, 2022. 2
- [28] Christoph Schuhmann, Romain Beaumont, Richard Vencu, Cade Gordon, Ross Wightman, Mehdi Cherti, Theo Coombes, Aarush Katta, Clayton Mullis, Mitchell Wortsman, Patrick Schramowski, Srivatsa Kundurthy, Katherine Crowson, Ludwig Schmidt, Robert Kaczmarczyk, and Jenia

- Jitsev. Laion-5b: An open large-scale dataset for training next generation image-text models, 2022. [4](#)
- [29] John Schulman, Filip Wolski, Prafulla Dhariwal, Alec Radford, and Oleg Klimov. Proximal policy optimization algorithms, 2017. [2](#)
- [30] Zhihong Shao, Peiyi Wang, Qihao Zhu, Runxin Xu, Junxiao Song, Xiao Bi, Haowei Zhang, Mingchuan Zhang, YK Li, Yang Wu, et al. Deepseekmath: Pushing the limits of mathematical reasoning in open language models. *arXiv preprint arXiv:2402.03300*, 2024. [2](#)
- [31] Jiaxin Shi, Kehang Han, Zhe Wang, Arnaud Doucet, and Michalis Titsias. Simplified and generalized masked diffusion for discrete data. *Advances in neural information processing systems*, 37:103131–103167, 2024. [2](#)
- [32] Yang Song, Prafulla Dhariwal, Mark Chen, and Ilya Sutskever. Consistency models. 2023. [2](#)
- [33] Keqiang Sun, Junting Pan, Yuying Ge, Hao Li, Haodong Duan, Xiaoshi Wu, Renrui Zhang, Aojun Zhou, Zipeng Qin, Yi Wang, Jifeng Dai, Yu Qiao, Limin Wang, and Hongsheng Li. Journeydb: A benchmark for generative image understanding, 2023. [S2](#)
- [34] Onkar Susladkar, Jishu Sen Gupta, Chirag Sehgal, Sparsh Mittal, and Rekha Singhal. Motionaura: Generating high-quality and motion consistent videos using discrete diffusion. *arXiv preprint arXiv:2410.07659*, 2024. [2](#)
- [35] Xiaoshi Wu, Yiming Hao, Keqiang Sun, Yixiong Chen, Feng Zhu, Rui Zhao, and Hongsheng Li. Human preference score v2: A solid benchmark for evaluating human preferences of text-to-image synthesis. *arXiv preprint arXiv:2306.09341*, 2023. [2](#)
- [36] Enze Xie, Junsong Chen, Junyu Chen, Han Cai, Haotian Tang, Yujun Lin, Zhekai Zhang, Muyang Li, Ligeng Zhu, Yao Lu, et al. Sana: Efficient high-resolution text-to-image synthesis with linear diffusion transformers. In *The Thirteenth International Conference on Learning Representations*, 2025. [2](#)
- [37] Jiazheng Xu, Xiao Liu, Yuchen Wu, Yuxuan Tong, Qinkai Li, Ming Ding, Jie Tang, and Yuxiao Dong. Imagereward: Learning and evaluating human preferences for text-to-image generation. *Advances in Neural Information Processing Systems*, 36:15903–15935, 2023. [2](#)
- [38] Yinan Zhang, Eric Tzeng, Yilun Du, and Dmitry Kislyuk. Large-scale reinforcement learning for diffusion models. In *European Conference on Computer Vision*, pages 1–17. Springer, 2024. [2](#)
- [39] Yulai Zhao, Masatoshi Uehara, Gabriele Scalia, Sunyuan Kung, Tommaso Biancalani, Sergey Levine, and Ehsan Hajiramezanali. Adding conditional control to diffusion models with reinforcement learning, 2025. [3](#)
- [40] Hongkai Zheng, Weili Nie, Arash Vahdat, and Anima Anandkumar. Fast training of diffusion models with masked transformers. *arXiv preprint arXiv:2306.09305*, 2023. [2](#)
- [41] Zhengbang Zhu, Hanyue Zhao, Haoran He, Yichao Zhong, Shenyue Zhang, Haoquan Guo, Tingting Chen, and Weinan Zhang. Diffusion models for reinforcement learning: A survey, 2024. [3](#)

## Supplementary Material

### A. Additional Experiment Results

Model	Step	Anime	Concept Art	Paintings	Photo	Overall
Baseline	16	28.401	27.508	27.539	27.149	27.649
Baseline	32	28.366	27.290	27.303	26.924	27.471
Baseline	48	28.179	27.122	27.094	26.771	27.292
Speed-RL	<b>16</b>	<b>28.441</b>	<b>27.643</b>	<b>27.443</b>	<b>27.261</b>	<b>27.697</b>
Speed-RL	32	29.653	27.730	27.613	27.384	27.845
Speed-RL	48	28.564	27.687	27.540	27.352	27.786

Table 4. HPSv2.0 Scores Comparison (Speed-RL vs. Baseline) by category for the HPS dataset.

Model	Step	Abstract	Animals	Artifacts	Arts	Food & Bev.	Illustrations	Indoor	Outdoor	Overall
Baseline	16	24.778	28.609	27.319	28.509	26.101	27.344	27.115	26.908	27.085
Baseline	32	24.273	28.498	27.396	28.138	25.896	27.358	27.008	26.724	26.911
Baseline	48	23.687	28.301	27.225	27.835	25.661	27.400	26.800	26.436	26.668
Speed-RL	<b>16</b>	<b>25.463</b>	<b>28.535</b>	<b>27.142</b>	<b>28.565</b>	<b>25.420</b>	<b>27.319</b>	<b>27.241</b>	<b>26.933</b>	<b>27.077</b>
Speed-RL	32	25.154	28.727	27.011	28.700	24.950	27.102	27.423	26.955	27.003
Speed-RL	48	24.919	28.602	26.842	28.627	24.778	27.027	27.394	26.792	26.873

Table 5. PartiPrompts Benchmark HPSv2.0 Scores (Speed-RL vs. Baseline) by Category. Speed-RL achieves a **+0.409** overall HPSv2.0 reward score with **3x** fewer steps than the baseline.

We evaluate Speed-RL across 16, 32, and 48 steps with the PartiPrompts Benchmark and HPS dataset using HPSv2.0 instead of v2.1. We previously had a minor labeling error and said v2.0 instead of v2.1. Because of this, we provide additional results for v2.0 in Table 4 and 5 (previous results were for v2.1). Overall, Speed-RL beats the Baseline scores for both benchmarks with fewer steps. In the HPS dataset, Speed-RL (16 steps) scores the highest on the Anime style. For the PartiPrompts dataset, Speed-RL (16 steps) scores the highest on the Animals category.

### B. Derivation of Loss

Recall that the standard GRPO loss is defined as

$$\mathcal{L}_{\text{GRPO-clip}} = \mathbb{E} \left[ \frac{1}{G} \sum_{i=1}^G \min \left( A_i r_i, A_i \text{clip} \left( r_i, 1 - \epsilon, 1 + \epsilon \right) \right) \right] - \beta \mathbb{D}_{\text{KL}}[p_\theta \| p_{\text{ref}}], \quad (5)$$

$$\text{where } r_i = \frac{p_\theta(x_i | c)}{p_{\text{old}}(x_i | c)}. \quad (6)$$

In fully online setup,  $p_{\text{old}} = p_\theta$ , so the clip is never applied. The loss simplifies to

$$\mathcal{L}_{\text{GRPO-noclip}} = \mathbb{E}[\frac{1}{G} \sum_{i=1}^G A_i r_i] - \beta \mathbb{D}_{\text{KL}}[p_\theta \parallel p_{\text{ref}}], \quad (7)$$

$$\text{where } r_i(c, x) = \frac{p_\theta(x_i | c)}{p_{\text{old}}(x_i | c)}. \quad (8)$$

We plug in our KL Estimator

$$\mathbb{D}_{\text{KL}}[p_\theta \parallel p_{\text{ref}}] = H(p_{\text{ref}} | p_\theta) - H(p_{\text{ref}}) \quad (9)$$

$$= \mathbb{E}_x[\sum_{i=1}^L \sum_{j=1}^{|V|} p_{\text{ref}}(x_i = j | c) \log p_\theta(x_i = j | c) - H(p_{\text{ref}})] \quad (10)$$

where  $L = HW$  is the number of image tokens and  $|V|$  is the VQ codebook size. This leads to

$$\mathcal{L}_{\text{GRPO-noclip}} = \mathbb{E}[\frac{1}{G} \sum_{i=1}^G A_i \frac{p_\theta(x_i | c)}{p_{\text{old}}(x_i | c)} - \beta \mathcal{L}_{ce}(p_{\text{ref}}(X_i, c), \log p_\theta(X_i, c))] \quad (11)$$

$$(12)$$

The entropy term,  $H(p_{\text{ref}})$  since it does not contribute to gradients. Now consider the gradient

$$\nabla_\theta \frac{p_\theta(x_i | c)}{p_{\text{old}}(x_i | c)} = \nabla_\theta \exp(\log p_\theta(x_i | c) - \log p_{\text{old}}(x_i | c)) \quad (13)$$

$$= \exp(\log p_\theta(x_i | c) - \log p_{\text{old}}(x_i | c)) \nabla_\theta (\log p_\theta(x_i | c) - \log p_{\text{old}}(x_i | c)) \quad (14)$$

$$= \exp(0) \nabla_\theta \log p_\theta(x_i | c) \quad (15)$$

$$= -\nabla_\theta \mathcal{L}_{ce}(\mathbf{x}_i, p_\theta(X_i | c)) \quad (16)$$

where  $\mathbf{x}_i$  is a one-hot vector. Hence, optimizing Eq. (12) is equivalent to optimize Eq. (4) in section Sec. 3.1. (Note that the Speed-RL is a minimizing objective, while GRPO is a maximizing objective, so the sign is flipped). Since cross entropy is linear in the first term, we further simplify the loss to the following in our implementation

$$\mathcal{L}_{\text{speed-rl}} = \mathbb{E}[\frac{1}{G} \sum_{i=1}^G \mathcal{L}_{ce}(A_i \mathbf{x}_i + \beta p_{\text{ref}}(X_i, c), \log p_\theta(X_i, c))] \quad (17)$$

$$(18)$$

Note that technically  $A_i \mathbf{x}_i + \beta p_{\text{ref}}(X_i, c)$  are not valid probability vectors as they do not sum to 1 at each token position. Hence,  $\mathcal{L}_{ce}$  is a mere algebraic notation rather than a true cross entropy between two probabilities.

## C. Datasets

We obtain the prompts for RL training from BLIP3o-60k [6] datasets, which contains the prompts from MSCOCO [17], JourneyDB [33], and other hand-crafted prompts. We visualize their distribution in Figure 8 and Table 6. We observe that the base model generates poor-quality images for extremely short prompts like ‘‘a person’’, which harms the training stability. Furthermore, we observed that prompts with only emojis and prompts with non-English text also harmed the training stability. Hence, we preprocessed the prompts and removed non-English prompts, prompts with only emojis, and prompts less than 7 words long.

Specifically, the prompts contain the following categories:

- **Randomly Sampled Prompts from JourneyDB.** These are long prompts with detailed descriptions of highly creative and complex scenes, such as characters from movies in different forms and styles and fictional backgrounds combining different elements. For example, "A skydiver from America in the 1970s is captured in a freefall pose, showcasing a mohawk hairstyle reminiscent of 'Weird Al' Yankovic's unique style. The skydiver daringly goes without a helmet, while the backdrop blends the futuristic cityscape of Dubai in 2023 with the contemporary skydiving trends. This realistic photograph, taken using a 35 mm lens on Kodakchrome film with ISO 800, f/4, and a shutter speed of 1/30, offers a breathtaking view in stunning 8k FullHD resolution."
- **Randomly Sampled Prompts from Dalle3.** These are long prompts describing an image in detail. For example, "The image showcases a character with a striking appearance. The character has a mohawk-style hairstyle with a vibrant pink hue. The side of their head is shaved, adorned with a metallic band that has a unique symbol on it. Their face is painted with bold red streaks, and they have piercings on their ears. The character is draped in a shiny, red cloak or garment. The background is a dilapidated, post-apocalyptic setting with rusted metal, broken windows, and a hazy atmosphere."
- **Randomly Sampled Prompts from MSCOCO.** These are captions from the MSCOCO dataset, which consists of real photos. For example, "A man riding a wave on a surf board" and "A woman is slicing a cake with her friends."
- **Randomly Sampled Prompts from GenEval.** These are prompts focused on objects and their properties like count, color, position, and co-occurrence. For example, "a photo of a white hair comb and a brown bear" and "a green zebra and a yellow cabinet."
- **Randomly Sampled Prompts from occupation\_1.txt and occupation\_2.txt.** These are prompts describing a human performing a specific occupation. For example, "An accountant in a crisp white shirt and tie, scanning through a computer screen filled with colorful bar graphs, while sipping a steaming cup of coffee in a modern office."
- **Randomly Sampled Prompts from object\_1.txt and object\_2.txt.** The first set of object prompts include a single object described in around 1 to 3 words, such as "Bar Soap" and "Toaster." The second set of object prompts include a description of a scene that may include more than one object. For example, "A close-up of thermometer and hex bolt on a table" and "A person holding curtain rod and engine piston in their hand."
- **Randomly Sampled Prompts from human\_gestures.txt.** These prompts describe humans performing different kinds of actions. For example, "Driving a car", "Opening a door", "Arriving at school", "Listening to music", and "Passing a basketball."

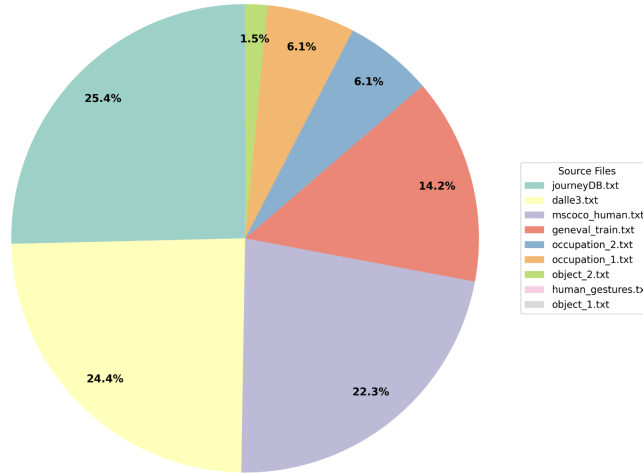


Figure 8. Distribution of selected prompt sources from BLIP3o-60k.

## D. Additional Qualitative Examples

We present additional side-by-side evaluation results in Figure 9. Examples 1 through 9 show a clear improvement in visual quality for Speed-RL (16 steps) compared to the baseline generation with 16 steps. Furthermore, for all nine examples, the 16 step Speed-RL generations are of comparable visual quality to the baseline 48 step generations. In fact, for Examples 7 and 8 Speed-RL's 16 step generations align with the prompt slightly better. In Example 7, Speed-RL's 16 step generation aligns better with key parts of the prompts such as "Maya-style housing" and "Winnie the Pooh." In Example 8, the prompt



Table 6. Distribution of prompt sources used from BLIP3o-60k.

<b>Source</b>	<b>Count</b>
journeyDB.txt	10,416
dalle3.txt	10,000
mscoco_human.txt	9,154
geneval_train.txt	5,848
occupation_2.txt	2,500
occupation_1.txt	2,500
Decsription of a scene involving several objects (object_2.txt)	625
human_gestures.txt	2
Single objects described in around 1 to 3 words (object_1.txt)	2
<b>Total</b>	<b>41,047</b>

says "blue sunglasses" which Speed-RL's 16 step generation correctly captures, but the baseline's 48 step generation does not (it generates orange sunglasses instead).

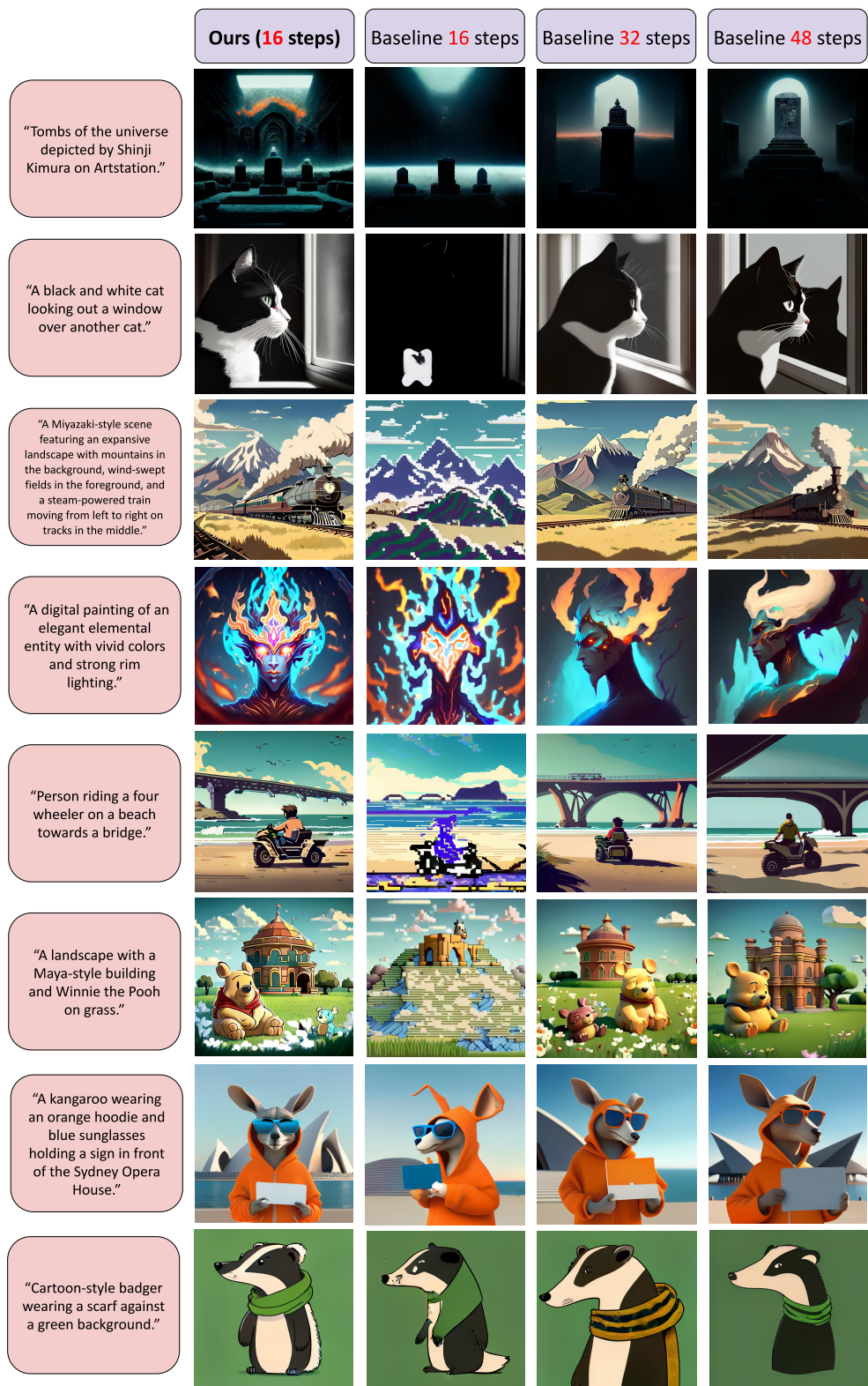


Figure 9. Additional side-by-side examples of Speed-RL with 16 steps and the baseline with 16, 32, and 48 steps.